Linearization of Nonlinear Components in Instruments

Clarence W. de Silva
The University of British Columbia
desilva@mech.ubc.ca

ABSTRACT

Real instruments, devices, and components are found to be nonlinear and are represented by nonlinear analytical models. Accordingly, linear systems (or models) have idealized representations. However, it is realized far more convenient to analyze, simulate, design, and implement nonlinear devices through the use of linear models. Also, regarding some devices, the degree of nonlinearity may not be significant. In such cases, nonlinear devices are often "approximated" by linear models. Against that background, this paper explores several important methods of linearization of nonlinear physical devices with practical examples.

KEYWORDS: *Nonlinear instruments, linearization methods, linearization using the local slope, linearization using energy equivalence*

1 INTRODUCTION

Real instruments and components are nonlinear (Chen and Chen 2013; Wang et al. 2011; Lang et al., 2017) and they may be represented by nonlinear analytical models. Linear systems (or models) are in fact idealized representations, and they are represented by linear differential equations in the time domain or by transfer functions of polynomial ratios in the frequency domain. It may not be possible to represent a highly nonlinear device by a single linear model in its entire range of operation. For small "changes" in response about some operating condition, a linear model may be used, which is valid in the assumed neighborhood of the operating condition. Commonly, linearization about an operating condition is done based on the "local slope" (or the first derivative) of the nonlinearity at the operating condition. Such linearization is not always feasible or satisfactory depending on the nature of the nonlinearity. Then, problem-specific and ad hoc approaches may have to be used to deal with system nonlinearities. The common methods of instrument linearization are the following (De Silva, 2023): slope-based analytical linearization over a limited range of operation about an operating condition (for both state-space models and input-output models); slope-based linearization using experimental input-output data (leading to experimental models); static linearization through recalibration or rescaling; linearization based on an equivalent model (using some criterion of equivalence such as energy); describing function method (this method also uses a criterion of equivalence—fundamental frequency component of the output); linearization using analog hardware; and feedback linearization.

This paper addresses two common methods of linearization: slope-based analytical linearization over a limited range of operation about an operating condition, and linearization based on an equivalent model through a criterion of energy equivalence. It presents two practical examples to illustrate these two methods of linearization.

https://doi.org/10.54389/KATU1803

2 NONLINEARITIES IN INSTRUMENTS

All physical devices are nonlinear to some degree. Broadly speaking, the nonlinear behaviour in instruments may be classified into two types: geometric (including kinematic) nonlinearity, specifically in a "mechanical" instrument, and physical (including kinetic) nonlinearity. Geometric nonlinearity stems primarily from large deflections or large motions, resulting in the introduction of nonlinear terms (e.g., trigonometric terms such as sine, cosine, and tan) in the representation of its input-output behavior. Kinematic relations of a robotic arm are an example of geometric nonlinearity. Physical nonlinearity results from the deviation from the linear (ideal) behaviour of its physical relations due to such causes as electrical and magnetic saturation, deviation from Hooke's law in elastic elements, plasticity, Coulomb and Stribeck friction, creep at joints, aerodynamic damping, backlash in gears and other loose components, and component wear out. Nonlinear Newton's 2nd law equation (i.e., kinetic nonlinearity) in a mechanical system also falls into the category of physical nonlinearity. Thus, many practical methods of linearization of instruments have been reported (Živanović, et al., 2004; Grützmacher, et al. 2018; Islam and Mukhopadhyay, 2019) Nonlinearities (particularly, physical nonlinearities) in devices are often manifested as some peculiar characteristics.

Saturation: Nonlinear devices may exhibit saturation (see Figure 1(a)). When saturated, the output of the device remains unchanged even when the input changes. This may be the result of causes such as magnetic saturation, which is common in magnetic-induction instruments, transformer-like instruments and other electro-magnetic instruments with a ferromagnetic core, differential transformers (in the current-magnetic field curve, where the magnetic field strength saturates); electronic saturation, as in amplifiers (in the input-output behavior, where the output saturates); elastoplastic behaviour in material (in the strain-stress curve, where the stress saturates as the strain increases); and in mechanical components like nonlinear springs (in the displacement-force curve, where the spring force saturates).

Ideal Relay: A special, ideal case of saturation is the "two-state *switching function*" or an *ideal relay*. In this case, the device saturates at two different (usually opposite) states, and does not have a linear (or variable) region in between. Then, the device can switch between these two states only.

Dead Zone: A dead zone is a region in which a device would not respond to an excitation (input). Stiction in mechanical instruments with Coulomb friction is a good example. Because of stiction, a component will not move until the applied force (input) reaches some minimum value. Once the motion is initiated, the subsequent behaviour can be either linear or nonlinear. Another example is the backlash in loose components such as gear wheels that do not mesh perfectly (where, the rotation is the input and the transmitted torque is the output). Bias signal in electronic instruments is a third example. In them, until the bias signal reaches a specific level, the circuit action will not take place, as in reverse bias of a diode until a breakdown (here, input is bias voltage, and output is transmitted current). A dead zone with subsequent linear behaviour is shown in Figure 1(b). In the case of stiction or Coulomb friction, if the input of the instrument is a motion (displacement or velocity) and the output is the corresponding force in the instrument, then the behaviour corresponds to an ideal relay (see under saturation) rather than a dead zone.

Hysteresis: Nonlinear devices may produce hysteresis. In hysteresis, the value of the input–output curve at a particular point becomes different depending on the direction of the input (see Figure 1(c)), resulting in a hysteresis loop. This behavior is common in loose components such as gears that have

backlash; in components with nonlinear damping, such as Coulomb friction; and in magnetic instruments or magnetic circuits (here, input is the magnetizing current, and output is the magnetic field strength) with ferromagnetic media and under various dissipative mechanisms (e.g., eddy current dissipation). For example, consider a coil wrapped around a ferromagnetic core. If a dc current is passed through the coil, a magnetic field is generated. As the current is increased from zero, the field strength will also increase. Now, if the current is decreased back to zero, the field strength will not return to zero because of the residual magnetism in the ferromagnetic core. A negative current has to be applied to demagnetize the core. It follows that the field strength vs. current curve looks somewhat like Figure 1(c). This is magnetic hysteresis.

The presence of a hysteresis loop alone does not imply that the instrument is nonlinear. For example, linear viscous damping also exhibits a hysteresis loop in its force–displacement curve. This is a property of any mechanical component that dissipates energy (then, area within the hysteresis loop = energy dissipated in one cycle of motion). In general, if force in a device depends on the displacement (as in the case of a spring) and the velocity (as in the case of a damping element), the value of the force at a given value of displacement will change depending on the direction of the velocity. In particular, the force when the component is moving in one direction (say positive velocity) will be different from the force at the same location when the component is moving in the opposite direction (negative velocity), thereby producing a hysteresis loop in the force–displacement plane. If the relationship of the displacement and velocity to the force is linear (as in viscous damping), the hysteresis effect is linear. If on the other hand the relationship is nonlinear (as in Coulomb damping and aerodynamic damping), the resulting hysteresis is nonlinear.

Hysteresis Loop and Energy Dissipation: When the two axes represent "force" and "displacement," it is known that the area of the hysteresis loop allows the net work to be done (or dissipated energy) in one cycle of movement. In this case, the input is the force and the output is the displacement. Note the loop arrows in Figure 1(c). Since "work done" is given by the integral of "force" × "incremental displacement," the area projected on to the *y*-axis (i.e., output axis or displacement axis) gives the work done. It is clear from Figure 1(c) that this area is greater in the forward direction of the loop (forward arrow) than in the backward movement. Hence, the net area is positive and is equal to the area of the hysteresis loop, indicating an overall net work done (or energy dissipation).

Jump Phenomenon: Some nonlinear instruments exhibit an instability known as the jump phenomenon (or *fold catastrophe*) in the frequency response (transfer) function curve that is determined experimentally. This is shown in Figure 1(d). As the frequency increases, the jump occurs from A to B; and as the frequency decreases, it occurs from C to D. In particular, note the bending of the resonant peak, corresponding to either a *hardening* instrument (where, the resonant frequency increases from the linear value, and the peak bends forward) or a *softening* instrument (where, the resonant frequency decreases from the linear value, and the peak bends backward). Furthermore, the experimentally determined transfer function of a nonlinear instrument may depend on the magnitude of the input excitation (The experimental transfer function of a linear instrument does not depend on the magnitude of the input).

Note: It should be clear that the segment AC in the nonlinear frequency response curve cannot be determined experimentally (it has to be determined either analytically or by interpolation of the experimental curve).

Limit Cycles: A notable property of a nonlinear system is that its stability may depend on the system inputs and/or initial conditions. In particular, nonlinear instruments may produce limit cycles.

An example is given in Figure 1(e) on the phase plane (2-D) of velocity vs. displacement. A limit cycle is a closed trajectory in the state space that corresponds to sustained oscillations at a specific frequency and amplitude, without decay or growth. The amplitude of these oscillations does not depend on the initial location from which the response started (unlike in a linear instrument). In addition, an external input is not needed to sustain a limit-cycle oscillation. In the case of a *stable limit cycle*, the response will move onto the limit cycle irrespective of the location in the neighborhood of the limit cycle from which the response was initiated (see Figure 4.1(e)). In the case of an *unstable limit cycle*, the response will move away from it with the slightest disturbance, and it follows that an unstable limit cycle cannot be determined experimentally.

Frequency Creation: A linear device, when excited by a sinusoidal signal, will generate a response at the same frequency as that of the excitation, at a steady state. On the other hand, at a steady state, a nonlinear instrument may create frequencies that are not present in the excitation signals. These created frequencies might be *harmonics* (integer multiples of the excitation frequency), *subharmonics* (integer fractions of the excitation frequency), or *nonharmonics*.

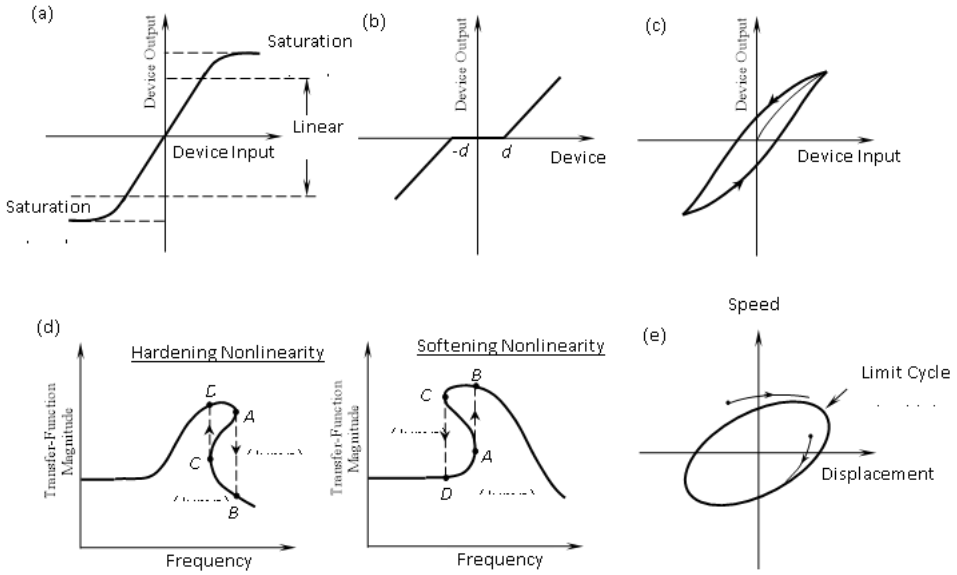

Figure 1. Common manifestations of nonlinearity in physical devices: (a) Saturation, (b) Dead zone, (c) Hysteresis, (d) Jump phenomenon, (e) Limit cycle response.

3 SLOPE-BASED LINEARIZATION

In the approach described now, linearization is carried out by determining the partial derivatives of the nonlinear terms, with respect to the independent variables, at the considered operating point. Typically, this linearizing point is the normal operating condition of the system. Of necessity, the normal operating condition has to be in a steady state or a equilibrium state.

3.1 Operating Condition in an Equilibrium State

In a steady state, by definition, the rates of changes of the system variables are zero. Hence, the steady state (equilibrium state) is determined by setting the time-derivative terms in the system equations to zero and then solving the resulting algebraic equations. This may lead to more than one solution, since

the steady-state (algebraic) equations themselves are nonlinear. The real (i.e., non-complex) steady-state (equilibrium) solutions will correspond to one of the following three types: 1. Stable (Here, given a slight shift, the system response eventually returns to the original steady state); 2. Unstable (Here, given a slight shift, the system response continues to move in the direction of the shift, away from the original steady state); 3. Neutral (Here, given a slight shift, the system will remain in the shifted condition). Next, the analytical linearization is illustrated using a practical example. This example involves a state-space model and an input-output model in two combined physical domains (mechanical and electrical). Hence, it is a multi-physics example.

3.2 Example of Slope-based Linearization

The robotic spray painting system of an automobile assembly plant employs an induction motor and pump combination, to supply paint at an overall peak rate of 15 gal/min to a cluster of spray-painting heads in several painting booths. The painting booths are an integral part of the production line in the plant. The pumping and filtering stations are in the ground level of the building and the painting booths are in an upper level. Not all booths or painting heads operate at a given time. The pressure in the paint supply line is maintained at a desired level (approximately 275 psi or 1.8 MPa) by controlling the pump speed, which is achieved through a combination of voltage control and frequency control of the induction motor. An approximate model for the paint pumping system is shown in Figure 2(a).

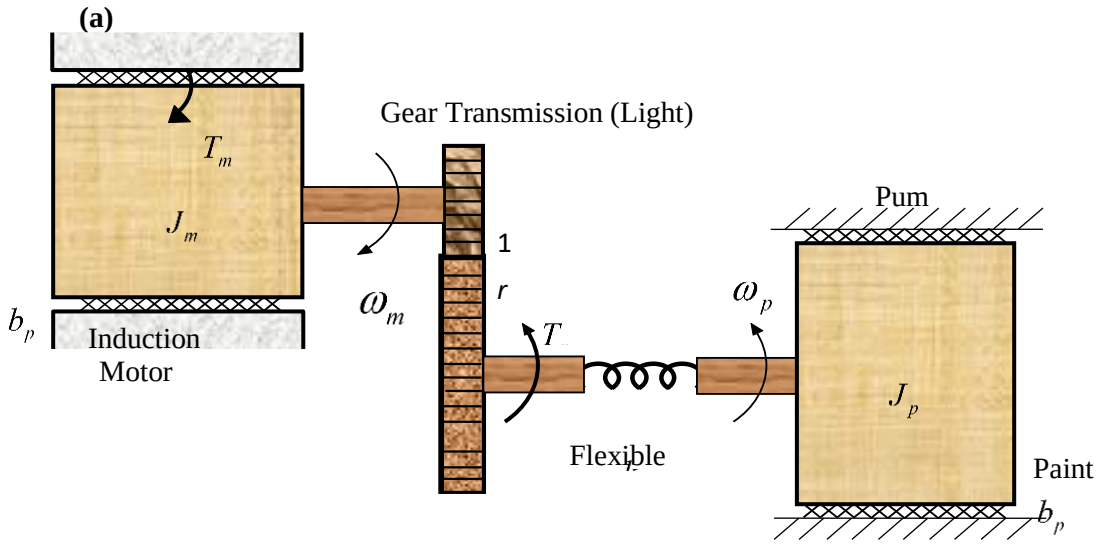

Figure 2. (a) A model of a paint pumping system in an automobile assembly plant;

(b)

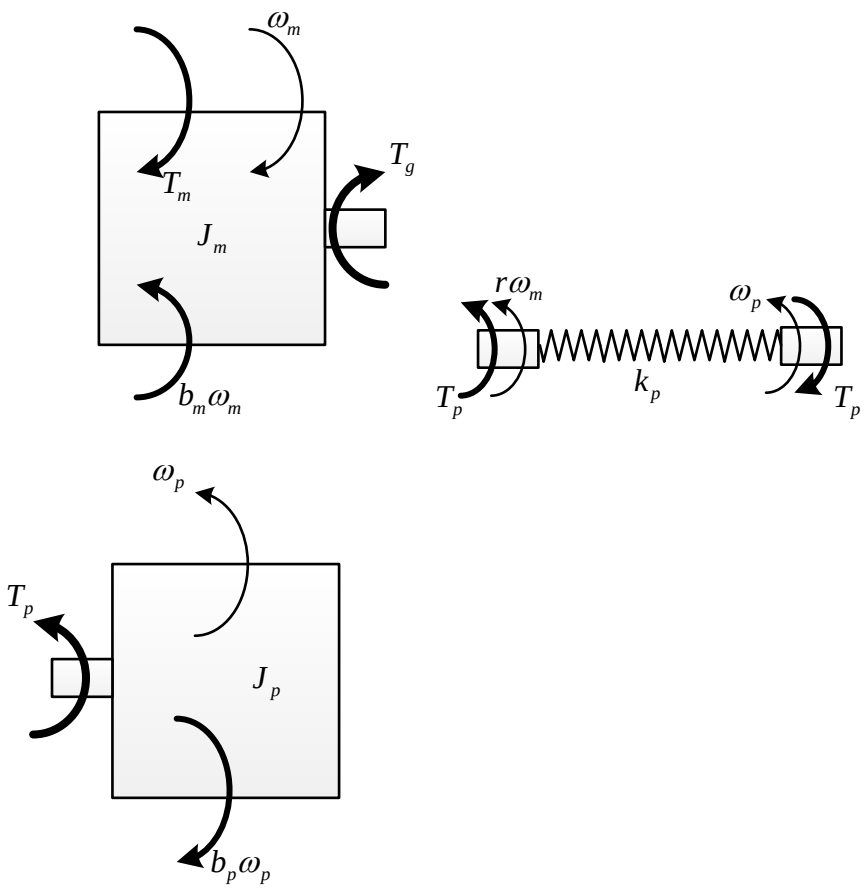

Figure 2. (b) Free-body diagrams of the energy storage elements.

The induction motor is linked to the pump through a gear transmission of efficiency η and speed ratio 1:*r* (a speed reducer is used, with *r* < 1), and a flexible shaft of torsional stiffness k_p. The moments of inertia of the motor rotor and the pump impeller are denoted by J_m and J_p, respectively. *Note*: The pump inertia J_p may include the "added-mass effect" of the paint. The gear inertia is neglected (or, if the dissipation is neglected, could be lumped with J_m, based on energy equivalence). The mechanical dissipation in the motor and its bearings is modelled as a linear viscous damper of damping constant b_m. The load on the pump (i.e., much of the paint load plus any mechanical dissipation) is also modelled by a viscous damper, and its equivalent damping constant is b_p. The magnetic torque T_m generated by the induction motor is given by

$$T_m = \frac{T_0 q \omega_0 (\omega_0 - \omega_m)}{(q\omega_0^2 - \omega_m^2)} \tag{1}$$

Here ω_m is the motor speed; the parameter T_0 depends directly (quadratically) on the phase (ac) voltage supplied to the motor; the second parameter ω_0 is the speed of the rotating magnetic field of the motor and is directly proportional to the line frequency of the ac supply; the third parameter q is greater than unity, and this parameter is assumed constant in the control system. Now, taking the motor speed ω_m, the pump-shaft torque T_p, and the pump speed ω_p as the state variables, the state equations for this (nonlinear) model are systematically derived.

In the steady-state operating condition of the system, suppose that the motor speed is steady at $\bar{\omega}_m$. We can obtain expressions for $\bar{\omega}_p$, $\bar{T}_p$ and $\bar{T}_0$ (at this operating point), in terms of $\bar{\omega}_m$ and $\bar{\omega}_0$. Voltage control of the motor is achieved by varying T_0 and frequency control by varying ω_0. The state model will be linearized about the operating condition and expressed it in terms of the incremental variables $\hat{\omega}_m$, $\hat{T}_p$, $\hat{\omega}_p$, $\hat{T}_0$, and $\hat{\omega}_0$. The (incremental) output variables are the incremental pump speed $\hat{\omega}_p$ and the incremental angle of twist of the pump shaft.

The nonlinearities of the device that are not included in the present model include the following: Backlash and inertia of the gear transmission have been neglected in the model. This assumption is not quite valid in general. Also, the gear efficiency η, which is assumed constant here, usually varies with the gear speed; Usually there is some flexibility in the shaft (coupling) that connects the gear to the drive motor; Energy dissipation (in the pump load and in various bearings) has been lumped into a single linear viscous-damping element. In practice, this energy dissipation is nonlinear and distributed; At least part of the pump load may be included as an "added inertia" to the pump rotor (usually this is not a constant). Alternatively, the pump load may be more accurately represented by a torque vs speed curve.

Now the state-space model of the device is derived. Let T_g = reaction torque on the motor from the gear. Output speed of the gear transmission is $r\omega_m$. Also, power = torque × speed. Hence, by definition, the gear efficiency is given by, $\eta = \dfrac{\text{Output Power}}{\text{Input Power}} = \dfrac{T_p r\,\omega_m}{T_g\,\omega_m}$. This gives, $T_g = \dfrac{r}{\eta}T_p$. The free-body diagrams for the energy storage elements are shown in Figure 1(b). There are two independent A-type elements and a T-type element in this device (De Silva, 2023). For them, the following three constitutive equations are written: Newton's 2nd law (Torque = Inertia × Angular Acceleration) for the motor:

$$J_m\dot{\omega}_m = -b_m\omega_m + T_m - T_g = -b_m\omega_m + T_m - \frac{r}{\eta}T_p \tag{2}$$

Here, we have substituted the previous result involving efficiency. Hooke's law (Torque rate = torsional stiffness × twisting speed) for the flexible shaft:

$$\dot{T}_p = k_p(r\omega_m - \omega_p) \tag{3}$$

Newton's 2nd law for the pump:

$$J_p\dot{\omega}_p = T_p - b_p\omega_p \tag{4}$$

Eqs. (2)-(4) are the three state equations, with the state vector $[\omega_m \quad T_p \quad \omega_p]^T$, which represent a "linear" model with input T_m. Strictly, the system is nonlinear with two inputs ω_0 and T_0 (note the torque-speed characteristic curve of the motor, given by eq (1) and sketched in Figure 3). Here ω_0 = speed of the rotating magnetic field of the motor (proportional to the line frequency), and T_0 depends quadratically on the phase voltage. Adjusting ω_0 corresponds to *frequency control* and adjusting T_0 corresponds to *voltage control*. The fractional slip *S* of the induction motor is,

$$S = \frac{(\omega_0 - \omega_m)}{\omega_0} \tag{5}$$

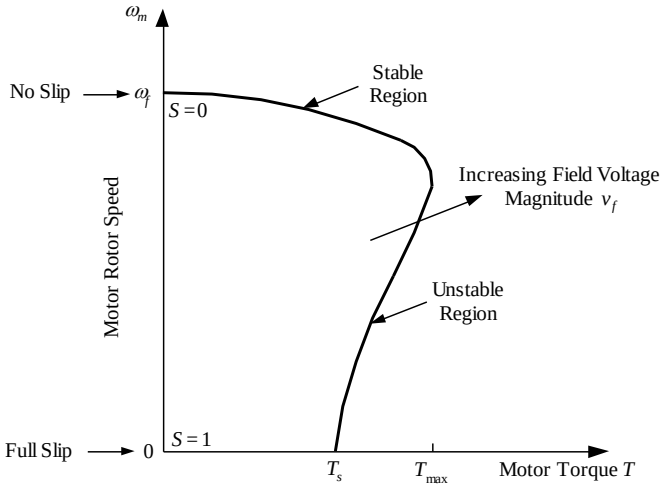

Figure 3. Torque-speed characteristic curve of an induction motor.

From eq (1) we note the following: When $\omega_m = 0$ we have $T_m = T_0$. Hence, T_0 = starting torque of the motor. When $T_m = 0$, we have $\omega_m = \omega_0$. Hence, ω_0 = no-load speed. This is the synchronous speed (Under no-load conditions, there is no slip in the induction motor, i.e., actual speed of the motor = speed ω_0 of the rotating magnetic field). Differentiate eq (1) separately wrt T_0, ω_0, and ω_m.

$$\frac{\partial T_m}{\partial T_0} = \frac{q\omega_0(\omega_0 - \omega_m)}{(q\omega_0^2 - \omega_m^2)} = \beta_1 \text{ (say)} \tag{6}$$

$$\frac{\partial T_m}{\partial \omega_0} = \frac{T_0 q[(q\omega_0^2 - \omega_m^2)(2\omega_0 - \omega_m) - \omega_0(\omega_0 - \omega_m)2q\omega_0]}{(q\omega_0^2 - \omega_m^2)^2} = \frac{T_0 q\omega_m[(\omega_0 - \omega_m)^2 + (q-1)\omega_0^2]}{(q\omega_0^2 - \omega_m^2)^2} = \beta_2 \tag{7}$$

$$\frac{\partial T_m}{\partial \omega_m} = \frac{T_0 q\omega_0[(q\omega_0^2 - \omega_m^2)(-1) - (\omega_0 - \omega_m)(-2\omega_m)]}{(q\omega_0^2 - \omega_m^2)^2} = -\frac{T_0 q\omega_0[(q-1)\omega_0^2 + (\omega_0 - \omega_m)^2]}{(q\omega_0^2 - \omega_m^2)^2} = -b_e \tag{8}$$

Since $q > 1$, we have $\beta_1 > 0$, $\beta_2 > 0$, and $b_e > 0$. b_e = electrical damping constant of the motor. In a steady state, the rates of changes of the state variables are zero. Hence set $\dot{\omega}_m = 0 = \dot{T}_p = \dot{\omega}_p$ in eqs. (2) – (4). We get $0 = \bar{T}_m - b_m\bar{\omega}_m - \frac{r}{\eta}\bar{T}_p$, $0 = k_p(r\bar{\omega}_m - \bar{\omega}_p)$, $0 = \bar{T}_p - b_p\bar{\omega}_p$.

Accordingly,

$$\bar{\omega}_p = r\bar{\omega}_m \tag{9}$$

$$\bar{T}_p = b_p r\bar{\omega}_m \tag{10}$$

$$\bar{T}_m = b_m\bar{\omega}_m + r^2 b_p\bar{\omega}_m/\eta = \frac{\bar{T}_0 q\bar{\omega}_0(\bar{\omega}_0 - \bar{\omega}_m)}{(q\bar{\omega}_0^2 - \bar{\omega}_m^2)} \quad \text{(from (1))}, \text{ or}$$

$$\bar{T}_0 = \frac{\bar{\omega}_m(b_m + r^2 b_p/\eta)(q\bar{\omega}_0^2 - \bar{\omega}_m^2)}{q\bar{\omega}_0(\bar{\omega}_0 - \bar{\omega}_m)} \tag{11}$$

The increment of the motor torque from the operating point is:

$$\hat{T}_m = \frac{\partial T_m}{\partial \omega_m}\hat{\omega}_m + \left[\frac{\partial T_m}{\partial T_0}\right]\hat{T}_0 + \left[\frac{\partial T_m}{\partial \omega_0}\right]\hat{\omega}_0 = -b_e\hat{\omega}_m + \beta_1\hat{T}_0 + \beta_2\hat{\omega}_0 \tag{12}$$

Take the increments of the state eqs. (2)-(4), and substitute (12). We get the linear state-space model:

$$J_m\dot{\hat{\omega}}_m = -(b_m + b_e)\hat{\omega}_m - \frac{r}{\eta}\hat{T}_p + \beta_1\hat{T}_0 + \beta_2\hat{\omega}_0 \tag{13}$$

$$\dot{\hat{T}}_p = k_p(r\hat{\omega}_m - \hat{\omega}_p) \tag{14}$$

$$J_p\dot{\hat{\omega}}_p = \hat{T}_p - b_p\hat{\omega}_p \tag{15}$$

State vector $\boldsymbol{x} = \begin{bmatrix}\hat{\omega}_m & \hat{T}_p & \hat{\omega}_p\end{bmatrix}^T$, Input vector $\boldsymbol{u} = \begin{bmatrix}\hat{T}_0 & \hat{\omega}_0\end{bmatrix}^T$, Output vector $\boldsymbol{y} = \begin{bmatrix}\hat{\omega}_p & \hat{T}_p/k_p\end{bmatrix}^T$

$$\boldsymbol{A}=\begin{bmatrix} -(b_e+b_m)/J_m & -r/(\eta J_m) & 0 \\ k_p r & 0 & -k_p \\ 0 & 1/J_p & -b_p/J_p \end{bmatrix};\quad \boldsymbol{B}=\begin{bmatrix} \beta_1/J_m & \beta_2/J_m \\ 0 & 0 \\ 0 & 0 \end{bmatrix};\ \boldsymbol{C}=\begin{bmatrix} 0 & 0 & 1 \\ 0 & 1/k_p & 0 \end{bmatrix};$$

$\boldsymbol{D}$ = **0;** b_e = electrical damping constant of the motor; b_m = mechanical damping constant of the motor.

In frequency control, $\hat{T}_0 = 0$. To get the linear input-output differential equation, we eliminate the state variables $\hat{\omega}_m$ and $\hat{T}_p$ from the state eqs. (13)-(15). We get:

$$J_m J_p \frac{d^3\hat{\omega}_p}{dt^3}+[J_m b_p + J_p(b_m+b_e)]\frac{d^2\hat{\omega}_p}{dt^2}+[k_p(J_m+\frac{r^2 J_p}{\eta})+b_p(b_m+b_e)]\frac{d\hat{\omega}_p}{dt}+$$
$$k_p(\frac{r^2 b_p}{\eta}+b_m+b_e)\hat{\omega}_p=\beta_2 r k_p \hat{\omega}_0 \qquad (16)$$

This is a 3rd order differential equation (the system is 3rd order, and the state-space model is 3rd order).

Observation from Result (16):

When $\hat{\omega}_0$ is changed by the "finite" step $\Delta\hat{\omega}_0$, the RHS of eq. (16) will change by a finite amount. Hence, the LHS also must change by a finite amount. In this process, suppose that lowest order term $\hat{\omega}_p$ instantaneously changes by a finite amount. That means, the higher order terms (higher derivatives) $\frac{d\hat{\omega}_p}{dt}$ and $\frac{d^2\hat{\omega}_p}{dt^2}$ have to change by "infinite" amounts, instantaneously (*Note*: The derivative of a step is an impulse—infinite). Then the LHS will change by an "infinite" amount, which violates the equation. Hence, only the highest derivative ($\frac{d^3\hat{\omega}_p}{dt^3}$) will change instantaneously. The lower derivatives will not change instantaneously.

The following somewhat general observations can be made from this example: 1. Mechanical damping constant b_m comes from bearing friction and other mechanical sources; Electrical damping constant b_e comes from the electromagnetic interactions in the motor, 2. The two damping parameters occur together (and should be treated together as a single unit, in analysis, simulation, design, control, etc.). For example, whether the response is underdamped or overdamped depends on the sum and not the individual damping parameters. This is a consequence of electro-mechanical coupling.

Note: If the characteristic curve corresponding to eq. (1) is experimentally determined, the damping parameter "*b*" that is determined from the curve, will contain mechanical damping (e.g., in bearings) as well since the torque is measured outside the bearings.

4 EQUIVALENT MODEL APPROACH OF LINEARIZATION

Another way to linearize a nonlinear model is through some criterion of equivalence. Here, a linear model that is equivalent to the nonlinear model is determined, based on some physical criterion. Approximating a distributed-parameter model by a lumped-parameter model by using energy equivalence is commonly done. Similarly, energy equivalence is a practical and convenient criterion of equivalence for linearizing a nonlinear device. Specifically, the energy absorbed (or dissipated, or work done) in executing a response cycle is used as the criterion for equating the two models. This approach is illustrated now using an example.

4.1 Example of Linearization based on Energy Equivalence

The nonlinear damper (e.g., a fluid damper) model (Figure 4(a)) has the constitutive relation,

$$f = c\dot{x}\,|\dot{x}| \tag{17}$$

Here, $f =$ damping force; $x =$ relative displacement; $\dot{x} = \dfrac{dx}{dt} =$ relative velocity; $c =$ damping parameter. When a harmonic (sinusoidal) force of frequency ω is applied to the damper, at steady state, the dominant sinusoidal component of the displacement will be $x = x_0 \sin(\omega t + \phi)$; $x_o =$ displacement amplitude, and $\phi =$ phase angle of the displacement with respect to the force.

For the linear viscous damper model (Figure 4(b)), the constitutive relation is,

$$f = b\dot{x} \tag{18}$$

Here, $b =$ viscous damping coefficient. Also, for both dampers,

$$x = x_0 \sin(\omega t + \phi) \tag{19}$$

$$\dot{x} = x_0 \omega \cos(\omega t + \phi) \tag{20}$$

For the nonlinear damper, energy dissipation per excitation cycle is, $\Delta u = \int\limits_{cycle} f\,dx = \int\limits_{cycle} f\,\dfrac{dx}{dt}dt$.

Substitute (17) and (20): $\Delta u = c\int\limits_{cycle} \dot{x}^2\,|\dot{x}|\,dt = cx_0^3\omega^3 \int\limits_{-\phi/\omega}^{(2\pi-\phi)\omega} \cos^2(\omega t + \phi)\,|\cos(\omega t + \phi)|\,dt$. Change variables: $\theta = \omega t + \phi$. Then, at $t = -\dfrac{\phi}{\omega}$, $\theta = 0$; At $t = \dfrac{(2\pi - \phi)}{\omega}$, $\theta = 2\pi$. Also, $d\theta = \omega dt$. Substitute:

$$\Delta u = cx_0^3\omega^2 \int_0^{2\pi} \cos^2\theta \left|\cos\theta\right| d\theta = 4cx_0^3\omega^2 \int_0^{\pi/2} \cos^3\theta d\theta \quad (Note: \cos\theta \geq 0 \text{ when } \theta = 0 \text{ to } \frac{\pi}{2})$$

$$= 4cx_0^3\omega^2 \int_0^{\pi/2} \cos\theta(1-\sin^2\theta)d\theta = 4cx_0^3\omega^2 \left[\sin\theta - \frac{1}{3}\sin^3\theta\right]_0^{\frac{\pi}{2}} = 4cx_0^3\omega^2(1-\frac{1}{3}) \quad .$$ Hence,

$$\Delta u = \frac{8}{3}cx_0^3\omega^2 \tag{21}$$

For the linear damper, as for the nonlinear damper,

$$\Delta u' = b \int_{cycle} \dot{x}^2 dt = bx_0^2\omega^2 \int_{-\phi/\omega}^{(2\pi-\phi)\omega} \cos^2(\omega t+\phi)dt = bx_0^2\omega \int_0^{2\pi} \cos^2\theta d\theta = bx_0^2\omega \int_0^{2\pi} \frac{1}{2}\left[1+\cos 2\theta\right]d\theta$$

$$= \frac{1}{2}bx_0^2\omega\left[\theta + \frac{1}{2}\sin 2\theta\right]_0^{2\pi} = \frac{1}{2}bx_0^2\omega \times \left[2\pi + 0\right] \quad \rightarrow$$

$$\Delta u' = \pi b x_0^2\omega \tag{22}$$

For the energy equivalence in one cycle, $\Delta u = \Delta u'$ with $b = b_{eq}$. Hence, $\pi b_{eq} x_0^2\omega = \frac{8}{3}cx_0^3\omega^2$, or,

$$b_{eq} = \frac{8}{3\pi}cx_0\omega \tag{23}$$

It is seen from the result (23) that the equivalent damping constant depends on both the excitation frequency and the response amplitude (hence on the excitation amplitude). This is a common characteristic of a nonlinear system and also seen in the describing function method. Therefore, the equivalent damping constant has to be changed during the use of this linear model, depending on the excitation frequency. The requirement that the equivalent linear model has the same displacement amplitude and frequency as the nonlinear damper, is not a limitation, as we deal with an "equivalent" model.

Note: At steady state (i.e., as $\omega \rightarrow 0$) $b_{eq} \rightarrow 0$, and the model will be able to provide very large speeds even with a very small excitation force. At very high frequencies (i.e., $\omega \rightarrow \infty$) $b_{eq} \rightarrow \infty$, and the model will not move. Both situations are quite realistic.

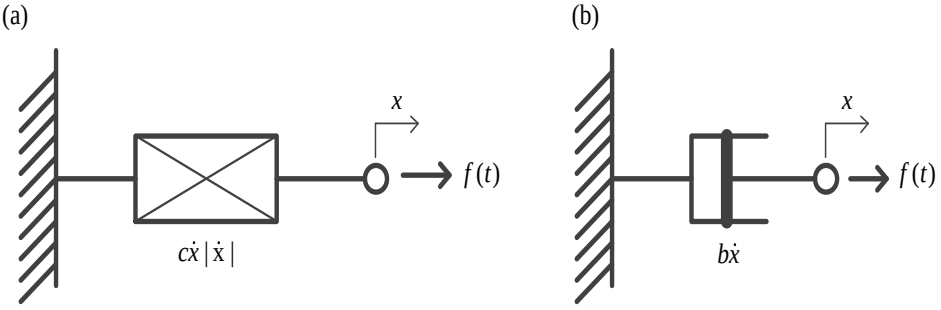

Figure 4. (a) A nonlinear fluid damper; (b) A linear viscous damper.

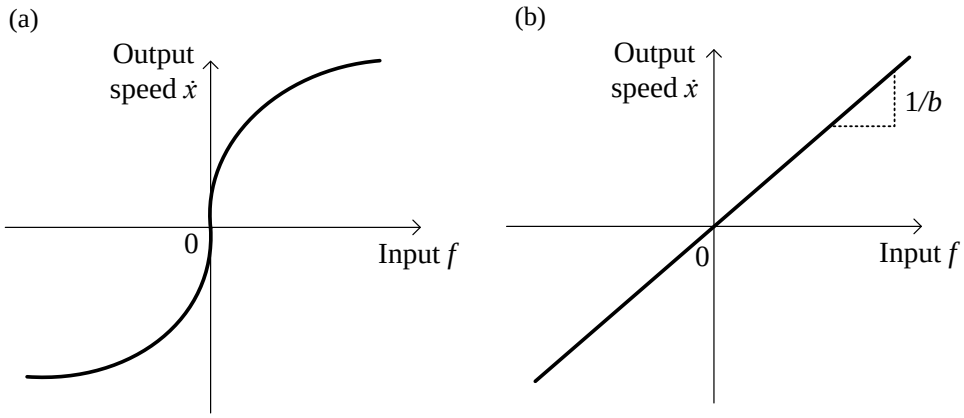

Figure 5. Damping behavior: (a) Nonlinear damping; (b) Linear viscous damping.

From the damping characteristics shown in Figure 5, it is clear that the nonlinear damping (Figure 5(a)) has an infinite slope at zero force (and at zero speed) unlike the linear viscous damping (Figure 5(b)), which has a finite slope. *Note*: Infinite slope means zero damping constant because, slope in Figure 5 is $\frac{\partial \dot{x}}{\partial f}$ while the damping constant is $\frac{\partial f}{\partial \dot{x}}$. Hence, local linearization (based on the local slope) is not practical in this type of nonlinear damping, particularly for low speeds (and low damping forces).

5 CONCLUSIONS

This paper addressed the linearization of nonlinear physical devices. In particular, the local slope-based linearization and the method that uses energy equivalence were examined. Illustrative examples of practical devices were analysed, to demonstrate the application of the two methods. Other possible methods of linearization were also indicated.

6 ACKNOWLEDGMENT

This work has been supported by the research grant RGPIN-2023-03243 from the Natural Sciences and Engineering Research Council (NSERC) of Canada.

REFERENCES

Chen, A. and Chen, C. (2013). Evaluation of piecewise polynomial equations for two types of thermocouples. *Sensors, Vol. 13(12),* pp. 17084–17097.

De Silva, C.W. (2023). *MODELING OF DYNAMIC SYSTEMS—With Engineering Applications*, 2nd edition, Taylor & Francis/CRC Press, Oxfordshire, UK.

Grützmacher, F, Beichler, B, and Hein, A. (2018). Time and memory efficient online piecewise linear approximation of sensor signals. *Sensors, Vo. 18(6),* pp. 1672-1691.

Islam, T and Mukhopadhyay, S.C. (2019). Linearization of the sensors characteristics: a review. *International Journal of Smart Sensors and Intelligent Systems, Vol. 12(1),* pp. 1–21.

Lang, H., Wang, Y., and de Silva, C.W. (2017). Semi-empirical Modeling and Parameter Analysis for the Development of a High Speed Resistance-welding Process. *International Journal of Modelling and Simulation, Vol. 38, No. 2,* pp. 1-9.

Wang, X, Wei, G, and Sun, J. (2011). Free knot recursive B-spline for compensation of nonlinear smart sensors. *Measurement, Vol. 44(5),* pp. 888–894.

Živanović, D, Arsić, M, and Djordjević, J. (2004). Two-stage piece-wise linearization method. *International Journal of Modeling and Simulation, Vol. 24(2),* pp. 85–89.